A. Falcione

Digital Computer Laboratory
Massachusetts Institute of Technology
Cambridge, Massachusetts

SUBJECT: NUCLEATION OF DOMAINS OF REVERSE MAGNETIZATION AND SWITCHING CHARACTERISTICS OF MAGNETIC MATERIALS

To: David R. Brown

From: J. B. Goodenough and N. Menyuk

Date: March 9, 1953

Abstract: The critical requirements for a ferromagnetic memory core are reviewed. Domains of reverse magnetization must form and grow within a core if its induction is to be reversed. The nature of the nucleation centers for these reverse domains will affect the shape of the hysteresis loop and the switching time. Inclusions, grain boundaries, and crystalline surfaces are analyzed as lattice imperfections which could act as nucleating centers. It is concluded that the grain boundaries are the most probable nucleation centers in most polycrystalline materials. It is shown that the criterion for a square hysteresis loop is $L(\cos\theta_1 - \cos\theta_2)^2 <$ Const. σ_w/I_s^2 where L is the average grain diameter, θ_1 and θ_2 are the respective angles made by the magnetization vector of two neighboring grains with the normal to their common surface, σ_w is the surface domain wall energy density, and I_s is the saturation magnetization of the sample. This explains why loops can be squared by the alignment of a direction of easy magnetization from grain to grain. It also reveals that materials which are not so aligned may have square loops if I_s is sufficiently small. The switching time τ for cores which are driven at fields roughly twice the coercive force (optimum operating conditions for a memory core) is related to the coercivity through the relation $H_c \tau = S_w$ where the switching coefficient S_w is a constant of the material. Experimental agreement with this model is found.

I. Introduction

In order to construct a satisfactory magnetic memory array[1] for

---

1. Jay W. Forrester, Jour. Appl. Phys., 22, 44 (1951)

a high-speed digital computer, it is necessary to obtain a magnetic material for the individual components which has: a) a small output signal ratio for a half to a full input pulse (or a square hysteresis loop); b) a short switching time; c) a low coercive force so that low driving currents can be used; d) a high flux density so as to give good output voltages; e) insensitivity to disturb, or half-amplitude, input signals; f) high uniformity of characteristics from core to core; and g) simplicity of manufacture of the individual units since millions of units will be required. The last of these requirements, and perhaps the second also, rules out the possibility of using single crystals which are cut into window frames with edges along the [100] directions of the crystal. These, although of academic interest, cannot be produced in sufficient quantities to be of practical use so that the strict requirements listed above must be found in a polycrystalline material.

The squareness of a hysteresis loop, which is measured by the squareness ratio $R_s = B_d/B_m$ (cf. Fig. 1), has been found in many materials to depend upon the degree of alignment of the axes of easy magnetization in the individual grains. These materials show a marked increase in R_s, for instance, after a magnetic anneal, grain orientation, or application of a tensile stress when these treatments tend to align the directions of easy magnetization parallel to the applied field.

The switching time, τ, of a magnetic core is defined as the time it takes to change the inductions in a core from $-B_r$ to B_m, or from B_r to $-B_m$, when a driving force H_m is applied. Experimentally time is measured from the moment the square driving pulse has risen to 10% of its amplitude. The output signal from the sensing winding, when plotted as a function of the time, has a double maximum. The time at which the output voltage has decayed to 10% of the voltage at the second maximum is τ (cf. Fig. 2). The initial rise time of the first maximum is limited by the rise time of the input pulse ($\sim$0.2 μsec) whereas the second maximum, which occurs only for driving forces $H_m > H_c$, moves to shorter times as the driving force is increased. At large driving forces, the resolution between the first and second maximum is lost. The output voltage of the "switching time curve" is a measure of the rate of change of flux in a magnetic core. According to magnetic domain theory, the flux change in a core is primarily a result of movement of domain or Bloch walls which are present in the material. When the flux in a magnetic core is reversed, or the core is "switched", walls must first be created within the

material, and then they must move through the core until they meet to annihilate one another or pass out of the material. The first maximum in the "switching time curve" appears to reflect the change of flux due to the creation of the domain walls and to reversible wall motion. The second maximum occurs only when $H_m > H_c$ so that irrevsible wall motion is taking place. Since the switching time τ, when $H_m > H_c$, is measured by the decay of the second maximum, it should be directly proportional to the distance the individual irrevsibly moving walls must move before the core is switched and inversely proportional to their velocity. The elementary walls do not all move the same distance when a core is switched. A distance ρ shall be defined as the distance a wall moving with the average velocity of the irrevsibly moving walls would move in a time τ. The average velocity will be inversely proportional to a damping factor β and directly proportional to the driving pressure on the wall. For a 180° wall the driving pressure is $2(H_m - H_o) \cdot I_s$. I_s is the saturation magnetization of the core. H_o is an average threshold field for the irrevsible motion of the irrevsibly moving walls whose motion causes the second maximum in the "switching time curve". If the motion of 180° domain walls predominates, the switching time, when $H_m > H_c$, will be

$$\tau \propto \rho \beta / 2(H_m - H_o) \cdot I_s. \qquad (1)$$

Because of the presence of eddy currents in metallic cores, thin ribbons of 1/8 mil thickness are used to reduce the damping factor β. At optimum operating conditions $(H_m - H_o) \approx H_c$. The low value of the coercivity in metallic ribbon cores limits the driving pressures which can be applied to a domain wall. The switching times in these materials are, consequently, long compared to those in the high-coercive force materials even though the saturation magnetization may be higher. There appear to be two possibilities of further reducing the switching time τ in the metallic ribbon cores. The first is to reduce the distance ρ by increasing the number of Bloch walls which move irreversibly in the material. The second, which is less desirable, is to increase the coercivity. The power restrictions on the driving currents impose an upper limit on the coercivity.

Disturb sensitivity of individual cores operating in a magnetic memory array appears to be the result of a coercivity which is small compared to that of the other cores in the array. Unless there is a high uniformity of coercivity among the cores, a core with lower coercive force than the others may have $H_c < H_m/2$. The pulsing currents are set for the array, not

for each individual core. If $H_c < 2/H_m$, however, the disturb pulse has sufficient amplitude to move the walls irrevsibly and destroy the information stored in the core.

The final requirement of high uniformity among the individual cores demands an understanding of the essential variables in a given material which effect its electro-magnetic properties and the preparation techniques which control these variables. At present the units are manufactured in large batches. Within each batch there is a statistical distribution of desired properties. The statistical mean varies from batch to batch. The testing and selection of millions of cores which meet the strict requirements of uniformity from these statistical distributions is a formidable prospect. It is hoped that a fundamental understanding of the variables and their control will greatly reduce the cost and effort in obtaining uniform magnetic units.

II. Nucleating Centers

In order to reduce the distance ρ in Equation (1), it is necessary to increase the number of domain walls which move irreversibly in the switching process; yet the remanence of the core should not be reduced any appreciable amount. This can be done only if the number of domain walls which are created at values of $H < H_m$ is increased. This increase, however, must not decrease the squareness ratio, R_s. When a ferromagnetic material is magnetically saturated, all of the elementary magnetic moments are aligned by the magnetic field and the sample contains no Bloch walls. If there were no imperfections in the crystal to act as nucleating centers for domains of reverse magnetization, the material would remain supersaturated, with no Bloch walls present, and the elementary magnets would have to rotate through a direction of difficult magnetization before the induction could be reversed. This is the type of supersaturation which exists in fine ferromagnetic powders[2] which exhibit extremely high coercivities. In large, polycrystalline samples, however, there are many imperfections in the lattice which might act as nucleating centers for domains of reverse magnetization. When a domain of reverse magnetization is created, it is encompassed by a 180° Bloch wall. The field strength at which a domain of reverse magnetization is created will be defined as H_n. The domain, once created, can grow to reverse the flux in the sample. The nucleating field strength, H_n, and the field strength which is necessary to move and expand the Bloch walls until the induction through the core vanishes, H_c, are smaller than that necessary to rotate all

---

2. C. Kittel, Phys. Rev. 70, 965 (1946).

of the elementary moments as a unit through a direction of difficult magnetization. In most materials $H_n < H_c$. In square-loop materials with vertical loop sides, however, it appears that $H_n > H_c$. Williams and Goertz[3] have examined this effect in a magnetically annealed perminvar ring. In this specimen $H_n \cong 2 H_c$. The exact mechanism of nucleation was not known. In order to reduce H_n, they notched the speciman. By introducing a nucleating center in the form of a notch, H_n was nearly halved. (The presence of the notch nucleated a domain of reverse magnetization in the specimen even at zero field strength. H_n is here taken at the field required to move the domain of reverse magnetization away from the imperfection which nucleated it. If a nucleation center is one to which a small domain of reverse magnetization is closely bound, H_n will be defined as the field strength required to liberate the small domain from the crystalline imperfection.) Thus the shape of the hysteresis loop for a magnetic specimen is critically dependent upon the nature of the crystal imperfections which act as nucleating centers for domains of reverse magnetization. If domains of reverse magnetization exist in a ferromagnetic material when a saturating d.c. field is reduced to zero, then the remanent induction in the material will be determined not only by the rotation of the magnetization vector of the individual grains to a direction of easy magnetization,[4] but also by the volume of material consisting of domains of reverse magnetization. The further creation and expansion of the domains of reverse magnetization as the magnetizing field is reversed cause a rounding off of the shoulder of the hysteresis loop. Materials with a high anisotropy constant should have minor hysteresis loops whose shapes are little affected by the rotation of the magnetization vector of the various individual grains. A principal influence on the remanent induction B_r and the squareness ratio R_s should be the domains of reverse magnetization. Square-loop materials (vertical sided dynamic loop) characteristically have a narrower static loop waist than loop shoulder and base. If, on the other hand, $H_n < H_c$ and the field required to create the different domains is significantly smaller over the various nucleating centers than the field required to produce their irreversible growth, the squareness ratio should be very poor.

---

3. H. J. Williams and M. Goertz, J. Appl. Phys. 23, 316 (1952).

4. R. M. Bozorth, Ferromagnetism, (D. Van Nostrand Company, Inc., New York 1951) p. 503.

Before the distance ρ and the nucleating field strength H_n can be controlled, it is necessary to examine those imperfections which occur in ferromagnetic materials which might act as the nucleating centers for domains of reverse magnetization.

The Grain Boundary

In a polycrystalline specimen the many grain boundaries are imperfections in the crystal lattice which could act as nucleating centers for domains of reverse magnetization. A crystal lattice is, in general, anisotropic with regard to ease of magnetization. If a crystal is not under tensile stress, this anisotropy is determined by the crystallographic configuration. As one goes across a grain boundary in a polycrystalline specimen, there is a change in crystallographic orientation and therefore a change in the directions of easy magnetization. Consequently at field strengths which are too low to rotate significantly the magnetization vectors out of a direction of easy magnetization, the component of the magnetization vector normal to the grain boundary will generally not be continuous across the grain boundary. Surface poles exist on the grain boundaries, and magnetic energy is associated with these surface poles. This magnetic energy would be reduced if domains of reverse magnetization existed to produce a surface pole distribution of alternating sign. Work must be done, however, in the formation of the domains of reverse magnetization. The grain boundaries will act as nucleating centers for domains of reverse magnetization only if the resulting reduction in energy associated with the grain boundary surface poles is larger than the work required to form the new domains.

In order to estimate the field strength H_n at which a grain boundary will act as a nucleating center for a domain of reverse magnetization, the problem is given definite specifications. Attention is focused on a section of grain boundary which can be considered planar and, therefore, to have a uniform distribution of surface pole density, $w^* = I_s (\cos\theta_1 - \cos\theta_2)$, where θ_1 and θ_2 are the angles made by the saturation magnetization vector I_s of the neighboring grains and the normal to their common boundary. It will be assumed that the applied field H is so small and the anisotropy constant K so large that the magnetization in any domain is directed along an easy axis of magnetization. It is further assumed that the section of grain boundary under consideration is far enough removed from the other grain boundaries of the material that interaction between their surface poles and the surface poles either on

the section of grain boundary under attention or associated with created Bloch walls are small compared to other energy considerations. It is also assumed that when nucleation occurs, it occurs periodically over the grain boundary plane with elementary area D^2. The domains of reverse magnetization are taken to be ovary ellipsoids of semi-major axis ℓ and semi-minor axis $R < D$ such that $\lambda = \frac{R}{\ell} \ll 1$ and the eccentricity is $e = \sqrt{1-\lambda^2} \approx 1$. Then the demagnetization factor of the new domain is $N \cong 4\pi\lambda^2\left[\ln\left(\frac{2}{\lambda}\right)-1\right]$, the volume of the new domain is $V = \frac{4\pi}{3} R^2 \ell$, and its surface area is $A_w = 2\pi\left(R^2 + \frac{R\ell}{e}\sin^{-1}e\right) \cong \pi^2 R\ell$. It should be noted that θ_1 and θ_2 are assumed small so that, since $\lambda \ll 1$, the two halves of the domain of reverse magnetization can be considered to have a common major axis in the estimation of N, V, and A_w. The change of internal energy of the crystal due to nucleation is then given by

$$\Delta E = (\sigma_o - \sigma_n) A - n\left[\sigma_w A_w + 2NI_s^2 V - HI_s(\cos\alpha_1 + \cos\alpha_2) V + E_p + E_{np}\right] \qquad (2)$$

where n is the number of domains of reverse magnetization nucleated on the area A of grain boundary under consideration. σ_w is the surface energy density of the 180° Bloch walls which are created, E_p is the interaction energy of the grain boundary poles with the poles associated with the new Bloch walls, and E_{np} is the interaction energy of the poles associated with the Bloch walls of neighboring domains. The demagnetization energy of each new domain is given by $\frac{1}{2}NI^2V = 2NI_s^2V$ since the surface poles associated with the Bloch walls are equivalent to those which would exist if the domains were in a vacuum with $I = 2I_s$. σ_o and σ_n are the surface energy densities of the grain boundary before and after nucleation has taken place. α_1 and α_2 are the angles the external field H makes with the directions of easy magnetization in the two neighboring grains.

If the x-axis is normal to the grain boundary plane and if a pill box is constructed on the plane, Gauss' Theorem gives $H_x = 2\pi\omega^*$ as the field associated with a uniform surface pole density ω^*. To calculate the surface energy density σ_o, it is assumed that the mean volume of a grain is L^3 so that an average value for σ_o would be

$$\sigma_o = \frac{1}{2}\int_0^L H_x I_s(\cos\theta_1 - \cos\theta_2)\, dx = \pi\omega^{*2} L$$

where account is taken of both sides of the grain boundary. σ_n, on the other

hand, can be calculated as outlined by Kittel.[5] Then

$$\sigma_n = \pi \sum_{-\infty}^{\infty} \sum_{-\infty}^{\infty} C_{mm} C_{-m-m} P_{mm}^{-1}$$

$$P_{mm} = 2\pi \sqrt{m^2 + m^2} / D$$

$$C_{mm} = \frac{1}{4\pi^2} \int_0^{2\pi} \int_0^{2\pi} \omega^*(\eta, \zeta)\, e^{-i(m\eta + m\zeta)}\, d\eta\, d\zeta$$

where $\eta = 2\pi y/D$ and $\zeta = 2\pi z/D$. for a circle of radius $R = D/b$ of surface pole density $-\omega^*$ imbedded in a square of side D of surface pole density ω^*, $\sigma_n = f(b)\omega^{*2} D$. Therefore

$$(\sigma_s - \sigma_n) A = n \left[\pi \left(\frac{1}{b}\right) - f(b) \right] D^3 \omega^{*2} \qquad (3)$$

In order to estimate E_p and E_{np}, it is noted that $\lambda \ll 1$. If, further, $R \ll D$, then the poles on the surface of the domains of reverse magnetization can be approximated by a line of poles along the major axis of the ovary ellipsoid of line density ρ_l^*. The equation of the ovary ellipsoid is

$$F(x, y, z) = \frac{x^2}{\lambda^2} + \frac{y^2 + z^2}{R^2} - 1 = 0$$

and the surface pole density is

$$\omega_d^* = I \frac{F_x}{\{F_x^2 + F_y^2 + F_z^2\}^{1/2}} = \frac{2 I_s \lambda x}{\{\lambda^2 - (1 - \lambda^2) x^2\}^{1/2}}.$$

Since $\lambda \ll 1$, the equivalent pole strength in the region between x and x + dx is

$$dm = \rho_l^* dx = 2\pi (y^2 + z^2)^{1/2} \omega_d^* dx \cong 4\pi I_s \lambda^2 x\, dx.$$

If it is further assumed that the major axis of the ovary ellipsoid is perpendicular to the grain boundary and that the primary contributions to E_p come from that portion of the grain boundary which is in the immediate neighborhood of the intersection of the domain of reverse magnetization, then if r is the radius vector from the foot of the major axis in the grain boundary plane,

$$E_p \approx \frac{1}{2} \iint \frac{\omega^*\, dS\, dm}{\sqrt{x^2 + r^2}} = \pi \iint \frac{\omega^* r\, dr\, \rho_l^*\, dx}{\sqrt{x^2 + r^2}}$$

5. C. Kittel, Rev. Mod. Phys. 21, 541 (1949).

where $\omega^* = |\omega^*| \begin{cases} -1 & \text{if } 0 \le r \le R \\ +1 & \text{if } R \le r \le D \end{cases}$.

This leads to

$$E_p \approx 8\pi^2 \left(\frac{b^2}{2} - 1\right) \omega^* I_s \lambda R^3 \quad \text{provided} \quad b\lambda \ll 1. \tag{4}$$

To estimate E_{np}, the two halves of the domain of reverse magnetization are assumed to have a common major axis. Each domain of reverse magnetization has four near neighbor domains a distance D away, and

$$E_{np} = 2\int_{-l}^{l} \rho_1^* dx_1 \int_{-l}^{l} \frac{\rho_{l2}\, dx_2}{\sqrt{D^2 + (x_2 - x_1)^2}} = 64\pi^2 I_s^2 \phi(d) \cdot \lambda R^3 \tag{5}$$

$$\phi(d) = 2\ln(2/d) - \tfrac{4}{3}\ln(1/d) - \tfrac{1}{18} + 2d + \text{terms in higher powers of d}$$

where $d = D/l = b\lambda$.

Equation (2) can be written, therefore, as

$$\Delta E = n I_s^2 \left\{ \gamma_g R^3 - a\gamma_\omega R l - \gamma R^3 \lambda + \gamma_H R^2 l \right\} \tag{6}$$

where the dimensionless parameters are

$$\gamma_g = \gamma_0 - \gamma_n = \left[\pi\left(\frac{L}{D}\right) - f(b)\right] l^3 (\cos\theta_1 - \cos\theta_2)^2,$$

$$\gamma = \pi^2 \left\{ \frac{32}{3}\left[\ln\left(\frac{2}{\lambda}\right) - 1\right] + 8\left(\frac{b^2}{2} - 1\right)(\cos\theta_1 - \cos\theta_2) + 64\phi(d) \right\},$$

$$\gamma_\omega = \frac{\pi^2}{a}\left(\frac{\sigma_\omega}{I_s^2}\right),$$

$$\gamma_H = \frac{4\pi}{3}\frac{H}{I_s}(\cos\alpha_1 + \cos\alpha_2),$$

and a is the distance between atoms whose magnetic moments give rise to the magnetization of the specimen. The logarithmic terms in γ should vary slowly with R compared to R and l themselves. Therefore since $n \propto 1/R^2$ and $L/D \propto 1/R$, the relation $\partial(\Delta E)/\partial R = 0$ gives, for the optimum value of R,

$$a\gamma_\omega / R = \gamma_n \lambda + 2\gamma\lambda^2.$$

If this relation is substituted into Equation (6), the condition that domains of reverse magnetization just form at the grain boundary is given by $\Delta E = 0$, $H = H_n$. Then

$$\gamma_{H_n} = 3\gamma\lambda^2 - (\gamma_0 - 2\gamma_n)\lambda. \qquad (7)$$

$\gamma_n \ll \gamma_0$ and $R \approx a\gamma_w / 2\gamma\lambda^2$ because $f(b) \ll \pi L/D$. Equation (7) therefore gives

$$H_n \approx \frac{3b^2\left\{\frac{3\pi\sigma_w}{2b^2\lambda} - L\omega^{*2}\right\}}{4I_s l(\cos\alpha_1 + \cos\alpha_2)}. \qquad (8)$$

It has been pointed out that if the grain boundaries are to be nucleating centers in a square hysteresis loop material, then $H_n \geq H_c$. The requirement that $H_n > 0$, however, gives the condition

$$L(\cos\theta_1 - \cos\theta_2)^2 < \frac{3\pi}{2b^2\lambda}\left(\frac{\sigma_w}{I_s^2}\right). \qquad (9)$$

The quantity L can be varied by altering the grain size. More significant, however, is the quantity $(\cos\theta_1 - \cos\theta_2)^2$ which can be varied by aligning the axes of easy magnetization of the various grains. This is done by annealing the specimen in a magnetic field, orienting the individual grains, or applying a tensile stress. It should be possible, therefore, to square the hysteresis loop and increase the remanence of a polycrystalline material by creating a single axis of easy magnetization provided the grain boundaries act originally as nucleating centers. 68 Permalloy is a particularly striking example of a polycrystalline material whose hysteresis loop is sensitive to tensile stress (cf. Fig. 4). In this material, the Curie temperature is $T_c = 873°K$, the anisotropy constant is $K \sim 10^4$ ergs/cm^3, the lattice parameter is $a = 2.5 \times 10^{-8}$ cm, and $I_s \sim 10^3$ so that

$$\left(\frac{\sigma_w}{I_s^2}\right) \approx \frac{1}{I_s^2}\left[\frac{RT_c \cdot K}{a}\right]^{1/2} \sim 10^{-7} \text{ cm}.$$

The ratio λ has been observed[3] to be about 0.04. Therefore if $L \sim 10^{-3}$ cm, condition (9) becomes

$$(\cos\theta_1 - \cos\theta_2)^2 < \frac{1.2}{b^2} 10^{-2} \sim 10^{-3}.$$

This condition is fulfilled only if $(\theta_1 - \theta_2) < 15^\circ$. The grain boundaries should, therefore, act as nucleating centers for domains of reverse magnetization in polycrystalline 68 permalloy. They can, however, be inhibited from becoming nucleating centers for low values of H_n by an alignment of the axes of easy magnetization from grain to grain in the direction of the applied external field. This can be done by the application of tensile stress σ.

It is concluded, therefore, that grain boundaries can and, in the case of 68 permalloy, do act as nucleation centers for domains of reverse magnetization. A significant feature of these nucleation centers is that they may be inhibited by aligning the axes of easy magnetization of the various individual grains. They should, to a lesser extent, also be sensitive to changes in the grain size of the material. More significantly, a small grain material should provide a larger area of grain boundary surface. This might provide a larger number of nucleated walls for a given H and reduce the distance ρ of Equation (1).

The Inclusion

In many lattices, especially in ferrites which are prepared by powder metallurgy techniques, there is a large density of inclusions present. These inclusions may be precipitates of a non-magnetic phase, impurity aggragates, or voids. Néel[6] predicted that in lattices with three axes of easy magnetization, closure domains are formed around the inclusions in order to reduce the energy associated with the magnetic poles at their surfaces. Williams[7] has observed these closure domains in colloidal maguetite patterns on polished surfaces of metals. He has also observed domains of reverse magnetization at large inclusions when there was only one axis of easy magnetization in the crystal.[3] One might therefore ask whether these small domains, which are known to form, can grow away from their nucleating inclusion in a magnetic field.

The principal resistance to the growth of a domain of reverse magnetization which is nucleated by an inclusion in a material with but one axis of easy magnetization is the inclusion surface pole density which caused its nucleation. The nucleating field strength, H_{n1}, in such a cyrstal will

---

6. L. Néel, Cahiers de Physique 25, 1 (1944).
7. H. J. Williams, Phys. Rev. 71, 646 (1947).

not, therefore, be defined as the field at which the domain forms. It is, rather, the field above which the domain can grow away from the nucleating inclusion. The domain will be free to grow away from the inclusion only when a second domain of reverse magnetization has been nucleated inside the first. [cf. Fig. 5(b).] The inner domain can grow to balance the poles on the surface of the inclusion as the original domain grows away from the inclusion. H_{n1} will be defined, therefore, as that field strength at which a second domain of reverse magnetization is nucleated inside the first. In order to estimate H_{n1}, it will be assumed that the inner domain forms with a base radius r_1 which is equal to the base radius of the domain which forms on a spherical inclusion of critical radius R_c. The critical radius is the smallest radius a spherical inclusion can have and nucleate a domain of reverse magnetization.

The energy associated with a spherical inclusion alone imbedded in a material of saturation magnetization I_s is given by its demagnetization energy

$$-\frac{1}{2}\int \underline{H}\cdot\underline{I}_s \, d\tau = \frac{1}{2} N I_s^2 \frac{4\pi}{3} R^3 = \frac{8\pi^2}{9} I_s^2 R^3.$$

The critical radius is that for which this energy just equals the energy of the configuration with a domain of reverse magnetization present. Since the energy of the new polar configuration about the inclusion will be to the old as a quadrupole term to a dipole term, it can, in first approximation, be neglected so that

$$\frac{8\pi^2}{9} I_s^2 R_c^3 = \sigma_w A_w + E_d \qquad (10)$$

where as before σ_w is the surface energy density and A_w the area of the created Bloch walls. E_d is the demagnetization energy of the domain of reverse magnetization. If the nucleated domain is an ovary ellipsoid of semi-minor axis r_1 and semi-major axis l_1, then

$$E_d = \frac{32\pi^2}{3}\left[\ln\left(\frac{2}{\lambda}\right) - 1\right] I_s^2 \lambda r_1^3$$

if $\lambda = r_1/l_1 << 1$. The value of r which gives an equal amount of positive and negative pole strength over an inclusion of radius R is $r = R/\sqrt{2}$. Therefore

$$E_d = \frac{16\pi^2}{3\sqrt{2}}\left[\ln\left(\frac{2}{\lambda}\right) - 1\right] I_s^2 \lambda R_c^3$$

$$A_w = \pi^2 r_1 l_1 = \pi^2 R_c^2 / 2\lambda$$

and Equation (10) gives

$$r_1 = R_c/\sqrt{2} = F(\lambda)\left(\frac{\sigma_w}{I_s^2}\right); \qquad F(\lambda) = \frac{9/16\,\lambda}{\sqrt{2} - 6\lambda\left[\ln\left(\frac{2}{\lambda}\right) - 1\right]}. \qquad (11)$$

If the minimum semi-minor axis of the inner nucleated domain in Fig. 8(b) is r_1 and the corresponding semi-minor axis of the outer nucleated domain is r_2 whereas it was r_0 when there was no field present, then H_{n1} can be derived from the energy balance

$$2 I_s H_{n1} \Delta V = \Delta(\sigma_w A_w) + \Delta E_d + \Delta E_p + E_{np} \qquad (12)$$

where E_p is the interaction energy between the poles associated with the Bloch walls and those on the inclusion surface and E_{np} is the interaction energy of the poles associated with the inner and outer Bloch walls. Attention is restricted to the case where the applied field H_{n1} is parallel to the direction of easy magnetization in the crystal. The increase in the volume of material magnetized parallel to H_{n1} is

$$\Delta V \approx \frac{4\pi}{3\lambda}\left\{r_2^3 - r_0^3 - r_1^3\right\}.$$

Since the estimates are necessarily of orders of magnitude only, it is assumed for simplicity that the parameter $\lambda = r_1/\lambda_1 = r_0/\lambda_0 = r_2/\lambda_2$. The change in demagnetization energy is

$$\Delta E_d \approx \frac{32\pi^2}{3}\left[\ln\left(\frac{2}{\lambda}\right) - 1\right] I_s^2 \lambda \left\{r_1^3 + r_2^3 - r_0^3\right\}.$$

The change in Bloch wall energy is

$$\Delta(\sigma_w A_w) \approx \frac{\pi^2 \sigma_w}{\lambda}\left\{r_2^2 - r_0^2 + r_1^2\right\} = \frac{\pi^2 I_s^2}{\lambda F(\lambda)} r_1 \left\{r_2^2 - r_0^2 + r_1^2\right\},$$

and the change in energy associated with the interaction of the poles on the surface of the inclusion is considered negligible compared to the other terms. If R is the radius of the inclusion, then $r_0 = R/\sqrt{2}$. If the integrated pole strength over the inclusion is zero, then $r_2^2 = r_1^2 + R^2/2$. r_1 is given by Equation (11). $r_1/R \ll 1$. Therefore

$$\Delta V \approx \frac{\pi}{\lambda} r_1^2 R \left\{\sqrt{2} - \frac{4}{3}\left(\frac{r_1}{R}\right)\right\}$$

$$\Delta(\sigma_w A_w) \approx \frac{2\pi^2 I_s^2}{\lambda F(\lambda)} r_1^3$$

$$\Delta E_d \approx 8\pi^2\left[\ln\left(\frac{2}{\lambda}\right) - 1\right] I_s^2 \lambda r_1^2 R \left\{\sqrt{2} + \frac{4}{3}\left(\frac{r_1}{R}\right)\right\}.$$

Since $\lambda << 1$, the poles associated with the Bloch walls will be approximated by lines of linear pole density $\rho_l^* = 4\pi I_s \lambda^2 \chi$. The inclusion surface poles can be approximated by a plane with concentric circles circumscribing regions of uniform surface pole density $\pm I_s$. Then

$$\Delta E_p = \frac{1}{2}\int_{-\frac{r_1}{\lambda}}^{\frac{r_1}{\lambda}}\int_S \frac{\omega^*(2)\, dS\, \rho_l^*\, d\chi}{\sqrt{\chi^2+r^2}} + \frac{1}{2}\int_{-\frac{r_2}{\lambda}}^{\frac{r_2}{\lambda}}\int_S \frac{\omega^*(2)\, dS\, \rho_l^*\, d\chi}{\sqrt{\chi^2+r^2}} - \frac{1}{2}\int_{-\frac{r_0}{\lambda}}^{\frac{r_0}{\lambda}}\int_S \frac{\omega^*(1)\, dS\, \rho_l^*\, d\chi}{\sqrt{\chi^2+r^2}}$$

where

$$\omega^*(2) = I_s \begin{cases} +1 & \text{for } \begin{cases} 0 \le r \le r_1 \\ r_2 \le r \le R \end{cases} \\ -1 & \text{for } r_1 \le r \le r_2 \end{cases} \qquad \omega^*(1) = I_s \begin{cases} -1 & \text{for } 0 \le r \le r_0 \\ +1 & \text{for } r_0 \le r \le R. \end{cases}$$

Integration yields

$$\Delta E_p = f_p(\lambda, r_1/R)\, I_s^2 r_1^3.$$

If the poles associated with the Bloch walls of the inner domain are approximated by a line charge and the outer is taken as a cone, then

$$\frac{1}{2} E_{mp} = \frac{1}{2}\int_S \int_0^{\frac{r_1}{\lambda}} \frac{\rho_{l_1}^*\, d\chi_1\, \omega_2^*\, dS_2}{\sqrt{(r_2-\chi_2\lambda)^2+(\chi_1-\chi_2)^2}}$$

where $\omega_2^*\, dS_2 = I_s \lambda \cdot 2\pi (r_2 - \chi_2 \lambda)\, d\chi_2$. Since $\lambda << 1$, this gives

$$E_{mp} = f_{mp}(\lambda, r_1/R)\, I_s^2 r_1^3.$$

The nucleating field strength defined by Equation (12) is, therefore,

$$H_{n1} = I_s \left\{ Q_1 + \left(\frac{r_1}{R}\right) Q_2\left(\lambda, \frac{r_1}{R}\right) \right\} \qquad (13)$$

where, if $r_1/R << 1$, $Q_1 = Q_1(\lambda)$. Williams and Goertz[3] have observed $\lambda \approx 1/30$ in a perminvar ring which was magnetically annealed. If this is taken as a representative value, then

$$H_{n1} \approx I_s \left\{ 4.31 \times 10^{-2} + \left(\frac{r_1}{R}\right) Q_2 \right\}. \qquad (14)$$

Q_2 is a positive quantity. When $r_1/R = 1/30$ and $\lambda = 1/30$, $r_1 Q_2/R \approx 3.3 \times 10^{-2}$ and $H_{n1} \approx 7.6 \times 10^{-2} \cdot I_s$. It is apparent, therefore, that if $I_s \sim 10^3$, as

in 68 permalloy, $H_{n1} \sim 70$ Oe. This is a large field compared to the usual coercivities in metals. Although domains of reverse magnetization are associated with inclusions of radius R_c or greater, it is concluded that these domains remain bound to the inclusion and are not responsible for the reversal of flux in a core with high I_s when it is switched at low field strengths. In materials of low I_s, such as the ferrites, however, these might be a contributing mechanism in the switching of the flux in a core with coercivities of the order of five oersteds.

In crystals with three axes of easy magnetization an inclusion, when there is no external field present, has closure domains associated with it as shown in Fig. 9(a).[6,7] In order for an inclusion with closure domains to act as a nucleating center for a domain of reverse magnetization, it is necessary for an external field, H_{n3}, to be applied which is strong enough to rotate the closure domains through forty-five degrees. The domain of reverse magnetization can then grow as shown in Figure 9. The field strength which is required to rotate a closure domain through an angle θ_1 is given by

$$H\left\{\int_0^{\theta_1}\int_{-l(\theta)}^{l(\theta)} \beta_l^*(l,\theta)\, l \sin\left(\tfrac{\pi}{4}-\theta\right) dl\, d\theta + I_s V \sin 2\theta_1\right\} = \tfrac{1}{4} K \sin^2 4\theta_1 + \Delta E_l + \Delta(\sigma_w A_w)$$

where K is the anisotropy constant. $V = \frac{4\pi}{3\lambda} a^3 \cos^3\theta_1$ is the volume of the domain after rotation through θ_1, a and l are the semi-minor and semi-major axes of the original closure domain, and $\lambda = a/l$ is assumed to remain constant. The change in demagnetization energy is

$$\Delta E_d = \frac{8\pi^2}{3} I_s^2 \lambda \left[\ln\left(\tfrac{2}{\lambda}\right) - 1\right] a^3 \left\{(1+\sin 2\theta_1)^2 \cos^2\theta_1 - 1\right\},$$

and the change in wall energy is

$$\Delta(\sigma_w A_w) = \frac{\pi^2 a^2}{\lambda} \sigma_w \left(\frac{\sigma_w(\theta_1)}{\sigma_w} \cos^2\theta_1 - 1\right).$$

Although the volume of the closure domain decreases as it is rotated to form a domain of reverse magnetization, it is assumed that no spins are rotated against the field direction. The change in volume is assumed to be absorbed in the increase in Bloch wall thickness. As the wall thickness increases, the surface wall density increases from σ_w to $\sigma_w(\theta_1)$.

In order to calculate the torque exerted by the interaction of the field with the poles associated with the Bloch walls, the surface poles are approximated by a linear pole density along the major axis of

$$\beta_l^* = 2\pi I_s \lambda^2 (1+\sin 2\theta)\, l.$$

If it is assumed that the anisotropy of the crystal offers the greatest resistance to rotation of the closure domain in the external field H, then the minimum nucleating field H_{n3} would be that which rotated the domain $\pi/8$ radius. When $\theta_1 = \pi/8$ and $\lambda = 1/30$,

$$H_{n3} = 0.324 \frac{K}{I_s} + 4.6 \times 10^{-2} I_s + 2.5 \frac{\sigma_w}{R I_s} \qquad (15)$$

where R is the mean radius of the inclusion. The optimum value of I_s for a small H_{n3} is given by setting $\partial H_{n3} / \partial I_s = 0$. This gives

$$I_s(op) \approx [7K + 54 \sigma_w / R]^{1/2},$$
$$H_{n3}(op) = 9.2 \times 10^{-2} I_s(op). \qquad (16)$$

For small K and large R a material might have $I_s(op) \sim 10^2$. The lowest value of H_{n3} is, therefore, about 10 Oe. This is larger than the usual coercive force H_c. Inclusions imbedded in lattices with three axes of easy magnetization will not act as nucleating centers for domains of reverse magnetization. Domains of closure will form and remain about the inclusions.

If a tensile stress of sufficient magnitude is applied to a ferromagnetic material whose grains originally posses three axes of easy magnetization, the resulting magnetostrictive forces will produce a single axis of easy magnetization either parallel or perpendicular to the applied stress. If inclusions are imbedded in the lattice matrix, their nucleating field strength for domains of reverse magnetization will change from H_{n3} to H_{n1}. The domains of closure will be rotated to become domains of reverse magnetization which can become free of the inclusion if a field $H > H_{n1}$ is applied parallel to the direction of easy magnetization. Since $H_{n3} > H_{n1}$, the application of a tensile stress will lower the field strength at which domains of reverse magnetization can be nucleated by an external field. If the nucleating centers are grain boundaries, however, Equation (8) shows that a tensile stress will raise the nucleating field strength. It appears, therefore, that if the hysteresis loop of a ferromagnetic specimen is squared by the application of a tensile stress, the nucleating centers in this material are grain boundaries.

The Crystal Surface

Every ferromagnetic lattice is bounded by its surface. If there were no internal defects to act as nucleating centers for a domain of reverse magnetization, the lattice would nevertheless not reverse its magnetization by a simultaneous rotation of all of its elementary magnetic moments unless it were so fine a particle that its diameter was equal to or less than the Bloch wall thickness. Instead, a Bloch wall would enter from the surface of the crystal and move across the specimen. The crystal surface is a third possible nucleating center for a domain of reverse magnetization. Both because the surface is irregular and because it is not, in general, parallel to the direction of easy magnetization in the adjacent grains, magnetic poles will exist along the surface of the specimen. These will act as nucleating centers in a manner analogous to the poles on the grain boundary surfaces. When the direction of easy magnetization in the various grains become perfectly aligned, the grain boundary surface poles disappear. A pole density will remain at the specimen surface, however, unless the surface is everywhere parallel to the easy magnetization direction.

In summary, of the three lattice defects which might be expected to nucleate domains of reverse magnetization, the grain boundaries and the surface of the specimen are the most likely. If the grain boundaries are responsible for nucleating domains of reverse magnetization, then the hysteresis loop squareness ratio R_s can be increased by aligning the axes of easy magnetization of the various individual grains. This is done in metals with a magnetic anneal or grain orientation. Neither of these methods is appropriate for the ferrites. If a ferrite has a large magnetostrictive constant, however, a tensile stress can align the axes of easy magnetization. Because $I_s \sim 10^2$ in the ferrites, condition (9) may be fulfilled even without the application of a tensile stress. If condition (9) is fulfilled, it will be possible to obtain relatively square hysteresis loops even without the application of an external stress provided $H_n \geq H_c$. H_n can be increased by decreasing L, or by decreasing the average grain size of the material. H_c can be reduced by greatly reducing the number of void inclusions. H_n can also be increased by increasing the anisotropy constant K and decreasing I_s with a variation of the alloying components of the ferrite. Since, according to Equation (1), the switching time is inversely proportional to I_s, it is

better to keep this quantity as large as possible, however. Of the ferrites currently under investigation, the nickel-zinc ferrites have low coercive force and poor squareness ratio. The squareness ratio can be greatly improved by the application of tensile stress which renders $H_n > 0$. The magnesium-manganese ferrites, on the other hand, have good squareness ratios without alignment of the axes of easy magnetization from grain to grain. The coercive force is large.

In a Sixtus-Tonks experiment the speed of propagation of the wave-front of reverse magnetization along a long rod of square-looped material is measured. Williams, Shockley, and Kittel[12] have suggested that the high values ($\sim 5 \times 10^4$ cm/sec/Oe.) for v/H in these experiments are a result of the small glancing angle which the moving wall makes with the propagation direction. If domains of reverse magnetization are nucleated as envisaged in this note, the small glancing angle is given by $\theta \approx \tan\theta = \lambda$. The Sixtus-Tonks experiment measures the rate of travel of a wave-front which consists of the apices of many domains of reverse magnetization which have been nucleated in one section of the specimen and grown until they collided with one another. The intercepted domains boundaries are annihilated; a jagged wave-front remains which travels down the length of the bar. The rate of travel of the wave-front is v/λ, where v is the velocity of the individual domain walls along their normal. The velocities from the Sixtus-Tonks measurements are greater than the domain wall velocity by the factor $1/\lambda$. When this factor is taken into account, the Sixtus-Tonks measurements are in good agreement with the theoretical wall velocity calculations and the direct measurements of wall velocity using colloidal magnetite techniques.

III. Switching Time

If the anisotropy constant in a material is large, the rotation of the elementary magnetic moments from a direction of easy magnetization will vary slowly with applied field strength. If the maximum field strength on a minor hysteresis loop is less than 2 Oe., the contribution of these rotations to the shape of the hysteresis loop will be small. The principal source of flux change must be domain creation and Bloch wall motion. The flux change due to either of these mechanisms may be reversible or irreversible. A schematic illustration of the four possibilities is given in Fig. 7. A potential curve for a 180° Bloch wall at zero field strength is indicated as a function of the position of the wall from the nucleating center along a normal to the wall. Fig. 7 (a) represents the Bloch wall potential when reversible nucleation takes place. If the material is placed in a field of sufficient strength to nucleate a wall, but not of sufficient strength to move the wall irreversibly through the crystal, $H_n < H < H_b$ where $H_c \approx H_b$ is the field required to move the wall over the first potential maximum, the wall will come to rest at some position x_a'. There will be a change in the induction of the sample due to the reversal of the magnetization vector in the volume enclosed by the created domain walls. When the field is removed, the wall returns to the nearest potential minimum. In this instance the created domain disappears and the material is in the same condition as before H was applied. Fig. 7 (b) represents the Bloch wall potential when irreversible nucleation takes place. If a field H, $H_n < H < H_b$, is applied, a domain of reverse magnetization will be nucleated and the domain wall will move to some position x_b'. When H is removed, the wall will return to the position x_b^o. The nucleated domain does not disappear. The induction in the sample at zero field before and after the field H is applied differs because of the reversal of magnetization in the irreversibly nucleated domain. There are various mechanisms which could be responsible for irreversible nucleation. Two of these are (1) the enclosure of an inclusion by the nucleated domain and (2) the meeting of two domains growing in opposite directions. The Bloch wall potential curves of Fig. 7 represent the case where $H_n < H_c$. If $H_n = H_c$, the wall potential at the nucleating center (x=0) would be the maximum point on the potential curve. An $H \geq H_n$ would nucleate a wall which would move irreversibly across the sample.

If a wall is already present at a position like x^o_b before a field $H < H_b$ is applied, the applied field will move the wall to some position x'_b. When the field is removed, the wall returns to x^o_b. There is no difference in induction at zero field before and after the field is applied. There is, however, a changing flux in the sample when the wall is moving reversibly one way or the other. If an $H > H_c \geq H_b$ is applied, both the nucleated walls and those already present will move irreversibly through the sample. If the driving field is cut off while the wall is moving through the crystal, the wall will settle into the nearest potential minimum. If the wall is at a position like x''_a when the field is shut off, the wall will stop and move backwards to its nearest minimum. If the wall is at a position like x''_b, it will continue moving forward to its potential minimum. It will very nearly reach this minimum within the fall-time of the driving pulse whereas walls caught at positions like x''_a will take a longer time to reverse their direction of motion to move back to a potential minimum. If, therefore, the same number of irreversibly moving walls are caught at x''_a positions as at x''_b positions when the driving field is shut off, their net contribution to the flux change after cut-off will be negative. The larger the area of irreversibly moving Bloch wall, the greater will be the negative change of flux associated with cut off. There will, of course, also be a negative change of flux associated with all reversible domain creations and wall movements when the driving field is cut off.

The "switching time curve" can be readily analysed on the basis of this model. Since the rise-time of the first maximum in this curve is the same as that for the input pulse, it is apparent that the walls are created and accelerated to their equilibrium velocity in less than the rise-time (0.2 μsec.). After the square driving pulse has risen to its maximum value, all the reversible motions will quickly stop. The loss of this contribution to the flux change will cause a decrease in the rate of change of flux in the sample. There should, therefore, be a maximum in the "switching time curve" at the time the input pulse reaches its full amplitude. This corresponds to the first maximum in the "switching time curve." The irreversibly moving walls will continue to move through the sample. These will have an average velocity which, for a constant driving field, should remain nearly constant once they have passed over their first potential maximum. If the average velocity of the walls which are contributing to the flux change is constant, the area of

wall which is moving must increase with time to a maximum and then decrease to zero if the rise to a second maximum with subsequent decrease to zero in the rate of change of flux curve, "switching time curve", is to be explained. This change in wall area, however, is just what is predicted by the picture of domain nucleation and growth. As the domains of reverse magnetization grow, the area of 180° domain wall increases until the separately nucleated domains begin to collide with one another. When a collision takes place, the common Bloch walls disappear. Collisions eventually reduce the area of the moving Bloch walls to zero. The second maximum in the "switching time curve", therefore, corresponds to the moment when the area of irreversibly moving Bloch wall is largest. It should be noted that this conclusion rests on the simple assumption that the large majority of irreversibly moving walls continue to move at a nearly constant average velocity until they are annihilated.

Quantitative Formulation

The equation of motion for a 180° domain wall moving perpendicular to an applied external field H is[8]

$$m\dot{v} + \beta v + \alpha \int v\,dt = 2\underline{I}_s \cdot \underline{H}. \qquad (17)$$

Galt[9] has found that in magnetite the inertial term $m\dot{v}$ is small compared to the viscous term βv. Since the rise to the first maximum in the "switching time curve" is determined by the rise-time of the input pulse in all materials tested, wall acceleration to an equilibrium velocity appears to occur in less than 10^{-7} sec. The inertial term is, therefore, neglected. A growing domain of reverse magnetization has a wall velocity

$$v = \dot{R}\sqrt{1+\lambda^2}/\cos\theta_i$$

where λ is the ratio of the minor to major axis of the growing domain. R is the component of the semi-minor axis on a cross-sectional plane through the magnetic sample and θ_i is the angle the direction of magnetization within the domain makes with the normal to this plane. Since $\lambda \ll 1$, Eq. (17) can be written

$$\beta\dot{R} + \alpha R = 2I_s H \cos\theta_i. \qquad (18)$$

The parameter α is a measure of the potential hills and valleys over which a Bloch wall moves. This elastic coefficient can be averaged over the various

8. R. Becker, J. Phys. et Radium, 12, 332 (1951)
9. J. K. Galt, Phys. Rev. 85, 664 (1952)

individual walls. If $d\langle R\rangle/dt$ is the rate of change of the mean R for all of the areas of reverse magnetization which are nucleated by the field H_m on a cross-sectional plane through the speciman during the reversal of flux through the core, then an H_o can be defined as that field for which $\langle d\langle R\rangle/dt\rangle \to 0$. This field will not be very different from the coercivity of the material when driven by an $H = H_m > H_c$. Eq. (18) becomes

$$\beta \frac{d\langle R\rangle}{dt} = 2I_s (H_m - H_o) \langle \omega^2 \theta_i \rangle \qquad (19)$$

When the switching time is measured, τ is defined as the time it takes for the flux change to reach 10% of its value at the second maximum of the "switching time curve". The time is measured from the moment the input pulse has risen to 10% of its maximum amplitude. Since Eq. (19) is valid only when $H = H_m$, the calculated value of τ will differ slightly from the measured value because of the finite rise-time of the input pulse. This effect will be more noticeable at high values of H_m, or small τ, since the rise time will be an appreciable fraction of τ. Also if $H_m \leq H_c$, Eq. (19) will break down. In the range of optimum operating conditions, however, Eq. (19) is a good first approximation. The rate of change of flux in the material is

$$\frac{d\Phi}{dt} = 2 \frac{d}{dt} \int \mathbf{B} \cdot d\mathbf{A} = 2 \langle \omega \theta_i \rangle B_s \frac{dA}{dt} .$$

The two enters because the flux change is the result of a reversal of magnetization in the speciman. The total area of reversed magnetization in the cross-sectional plane is $A = \sum_i A_i$ where the A_i represents the contributions from the individual domains. These areas originate on the cross-sectional plane at different times and grow at different rates. If n is the total number of A_i which appear and grow on the cross-sectional plane when the core is "switched", then $A(t) = n f(\langle R\rangle)$ where $\langle R\rangle$ is a function of time. If a distribution function $F(\langle R\rangle) = n \, \partial f / \partial \langle R\rangle$ is defined, then

$$\frac{d\Phi}{dt} = 2\langle \omega \theta_i \rangle B_s F(\langle R\rangle) \frac{d\langle R\rangle}{dt} = \frac{16\pi I_s^2}{\beta} \langle \omega \theta_i \rangle \langle \omega^2 \theta_i \rangle F(\langle R\rangle) \left[H_m - H_o\right]. \qquad (20)$$

There are two factors which contribute to the viscous damping factor $\beta = \beta_r + \beta_e$. The first of these is the relaxation contribution, β_r, which arises from the sluggish response of the spins to a force which would change their direction. The second, β_e, is the eddy current contribution. Kittel[10] has indicated the essential features in the calculation of the viscous parameter β_r. Since $\lambda << 1$, the velocity of the Bloch walls will be essentially that of a cylindrical wall everywhere parallel to the direction of magnetization. Although Kittel's calculation is for a plane wall perpendicular to the z-axis moving in the z-direction, his formalism holds equally well for a cylindrical wall provided the variable $R/\cos\theta_i$ replaces the variable z, and the integrations are taken from zero to infinity. The rate of change of $\langle R \rangle$ which is limited by β_r becomes

$$\frac{d\langle R\rangle}{dt} = \frac{4A\left[\Lambda^2 + I_s^2\gamma^2\right](H_m - H_0)}{I_s \Lambda \sigma_w}\langle \cos^2\theta_i \rangle$$

where Λ is the intrinsic relaxation frequency which can be estimated from the line width in a microwave experiment. H is defined by the phenomenological equation of motion for the magnetization $\underline{I}$,

$$\frac{d\underline{I}}{dt} = \gamma \underline{I} \times \underline{H} - \Lambda\left\{(\underline{H}\cdot\underline{I})\underline{I}/I^2 - \underline{H}\right\}.$$

$\gamma = ge/2mc$ is the gyromagnetic ratio. σ_w is the rest energy of the 180° Bloch wall, and A is the usual exchange factor[5]. If the value of $d\langle R\rangle/dt$ from Eq. (19) is used, the relaxation contribution to the viscous parameter is given by

$$\beta_r = \frac{I_s^2 \Lambda \sigma_w}{2A(\Lambda^2 + I_s^2\gamma^2)} \qquad (21)$$

The calculation of σ_w for a cylindrical wall is similar to that given by Kittel[5] for a plane wall. If only interactions between nearest neighbors are considered, and if these interactions are all equal, the change in exchange energy due to the presence of a wall in which neighboring spins make a small angle $\phi_{ij} < 1$ is

$$\Delta W_{ex} \simeq JS^2 \sum_{i<j} \phi_{ij}^2$$

10. C. Kittel, Phys. Rev. 80, 918 (1950)

where J is the exchange integral and S is the total spin quantum number. J is so defined that for two spins 1/2 the energy for parallel orientation is lower than that for anti-parallel orientation by an amount 2J. If the crystal has only one axis of easy magnetization, the small angle can be expanded as

$$\phi_{ij} = r_{ij}\left(\frac{\partial \phi_{ij}}{\partial r}\right) + \frac{1}{2} r_{ij}^2 \left(\frac{\partial^2 \phi_{ij}}{\partial r_{ij}^2}\right) + \cdots$$

where r_{ij} is the component of the near-neighbor distance along the radius from the axis of the cylindrical domain to the i^{th} atom. If the axis of the cylindrical domain is along a cubic axis, and if θ is the angle between the radius to the i^{th} atom and a radius parallel to a cubic axis in a b.c.c. lattice, the i^{th} atom has four near neighbors with $|r_{ij}| = \frac{a\sqrt{2}}{2} \cos\left(\frac{\pi}{4} - \theta\right)$ and four with $|r_{ij}| = \frac{a\sqrt{2}}{2} \cos\left(\frac{\pi}{4} + \theta\right)$ where a is the length of a cube edge. Higher powers of the expansion can be neglected. Then

$$\sum_{i>j} \phi_{ij}^2 = \sum_{i>j} r_{ij}^2 \left(\frac{\partial \phi}{\partial r}\right)^2 = 2a^2\left[\cos^2\left(\frac{\pi}{4} - \theta\right) + \cos^2\left(\frac{\pi}{4} + \theta\right)\right]\left(\frac{\partial \phi}{\partial r}\right)^2.$$

There are two atoms per unit cell, and interactions must not be counted twice. The exchange energy density, therefore, is

$$f_{ex} = \frac{\Delta w_{ex}}{a^3} = A\left(\frac{\partial \phi}{\partial r}\right)^2$$

where the exchange parameter is $A = 2JS^2/a$. Since a single axis of easy magnetization has been assumed, the anisotropy energy density is $f_k \cong K_1 \sin^2\phi = G(\phi)$, where K_1 is the anisotropy constant. The surface energy density of a cylindrical wall of radius R is, therefore,

$$\sigma_w = \frac{1}{R}\int_0^\infty \left[f_k + f_{ex}\right] r\, dr \cong \int_0^\infty \left[G(\phi) + A\left(\frac{d\phi}{dr}\right)^2\right] dr$$

The assumption has been made that R is much greater than the wall thickness over which $\left[f_k + f_{ex}\right] \neq 0$. Minimization of the integral gives $f_k = f_{ex}$ and therefore

$$\sigma_w \cong 2(K_1 A)^{1/2} \int_0^\pi |\sin\phi|\, d\phi = 4(K_1 A)^{1/2}.$$

The relaxation contribution to the viscous parameter can now be expressed as

$$\beta_r = \frac{2 I_s^2 \Lambda}{(\Lambda^2 + I_s^2 \gamma^2)} \sqrt{\frac{K_1}{A}} \simeq \frac{2 I_s^2 \Lambda}{(\Lambda^2 + I_s^2 \gamma^2) S} \sqrt{\frac{a z K_1}{2 k T_c}} \qquad (22)$$

where T_c is the Curie temperature, and k is the Boltzmann gas constant. In first approximation z is the number of nearest neighbors with which exchange interaction occurs. Weiss[11] has calculated z for various lattices by an extension of the Bethe-Peierls method. It should be noted that although σ_w was calculated for a b.c.c. lattice, the wall energy density for the more complicated spinel lattice will only introduce a different numerical factor. Eq. (22) will, in first approximation, give a good value for β_r for all lattices provided the phenomenological equation defining Λ in Kittel's[10] calculation is valid.

A study of the velocity of a collapsing cylindrical domain wall in a cylindrical metal in which $\beta = \beta_e$ has already been made.[12] The analysis for a cylindrical wall of radius R in a cylindrical speciman of radius R_m which is expanding with a radial velocity $\dot{R}$ in a material of electrical resistivity ρ_e and saturation magnetization I_s is completely analogous. Since these authors were considering the case for high driving fields only, they equated the power dissipated by eddy currents, A, to the power generated by the alignment of flux with the driving field, B. For low field-strength it is necessary to include the power dissipated in overcoming the potential barrier to wall movement, C. The relation A + C = B gives

$$\dot{R} = (H_m - H_0)/\rho_e c^2 \cos^3\theta_i \,/\, 32\pi^2 I_s R \ln(R_m/R). \qquad (23)$$

In a rectangular specimen, such as a metallic ribbon core, $2R_m$ should be taken as the smaller dimension in the cross-sectional plane perpendicular to the flux path. Although there are many nucleated domains which are expanding so that the eddy currents between moving walls tend to cancel one another, there is no cancellation of the eddy currents near the surface of the core. Elimination of

---

11. P. R. Weiss, Phys. Rev. 74, 1493 (1948)
12. Williams, Shockley, Kittel, Phys. Rev. 80, 1090 (1950)

$d\langle R\rangle/dt$ from Eqs. (23) and (19) gives

$$\beta_e \cong \beta_e^{\circ} \frac{\langle R\rangle}{\langle \cos\theta_i\rangle} \ln\langle R_m/R\rangle \tag{24}$$

$$\beta_e^{\circ} = 4\pi^2 I_s^2/\rho_e c^2.$$

If the finite rise time of the square driving pulse is neglected, $(H_m - H_o)$ is time independent. Integration of Eq. (19) gives

$$(H_m - H_o)\tau = S_w \cong \frac{\rho\beta_r}{2I_s\langle\cos\theta_i\rangle} + S_w^e \tag{25}$$

$$S_w^e = \frac{\beta_e^{\circ}}{8I_s\langle\cos\theta_i\rangle} \begin{cases} \rho^2\{2\ln(R_m/\rho\langle\cos\theta_i\rangle) + 1\} & \text{if } \rho\langle\cos\theta_i\rangle \le R_m \\ \dfrac{R_m^2}{\langle\cos^2\theta_i\rangle} & \text{if } \rho\langle\cos\theta_i\rangle \ge R_m . \end{cases}$$

S_w is defined as the switching coefficient. It is a constant which depends upon the properties of the material in the core. The fraction $\langle\cos\theta_i\rangle/\langle\cos^2\theta_i\rangle$ is taken as $\langle\cos\theta_i\rangle^{-1}$ since small angles are involved. Galt[9] has found $\beta_e/\beta_r \cong 1/6$ in a single crystal of magnetite. This ratio is made small in the metallic tape cores by rolling them to 1/8 mil thickness. In the ferrites which have resistivities of a factor of 10^9 greater than magnetite the ratio will be extremely small. The switching time is, therefore, determined almost exclusively by the relaxation contribution and

$$(H_m - H_o)\tau = S_w \cong \frac{\rho I_s \Lambda}{(\Lambda^2 + I_s^2\gamma^2)S\langle\cos\theta_i\rangle}\sqrt{\frac{a \pm k_1}{2kT_c}} \tag{26}$$

The value of β_r from Eq. (22) has been used. If fast switching cores with low coercive force are to be found, S_w must be made smaller than 10^{-7} Oe-sec.

Comparison with Experiment.

H. K. Rising of this laboratory drove a 4-79 Mo-Permalloy ribbon core rolled to a thickness of 1/8 mil with a series of square pulses. The pulse amplitudes were all equal and of sufficient magnitude to switch the core. The first pulse was long enough for the core to switch completely. The succeeding series of pulses were 0.7 μ sec. long in the opposite direction. The core switched partially during each short pulse. It became fully switched only after the total time represented by the sum of several short pulses just exceeded the time for switching when driven by one long pulse. The oscilloscope trace is reproduced in Fig. 8. The "switching time curve" for the first long pulse shows the usual double maximum. The rise to the first maximum occurs during the rise of the input pulse. The interesting feature of this experiment is that the second maximum of the "switching time curve" is almost completely dependent upon the state of magnetization of the specimen. The small "bits" from the successive 0.7 μ sec. pulses, if pieced together, nearly trace out the curve resulting from one long pulse. This follows directly from the model of nucleated domains which grow irreversibly to switch the core. If the second maximum were the result of an increase in velocity of domain walls with fixed area, there would not be this dependence on the state of magnetization of the core. According to the model of this paper, the rate of change of flux which contributes to that part of the curve which is due to irreversible wall motion is, by Eq. (20), proportional to $F(\langle R \rangle)$. $F(\langle R \rangle)$ represents the change of flux in the sample with respect to the change in position of the walls. It increases to a maximum when the wall area encompassing the growing domains is a maximum. Because of the random distribution of the nucleated domains throughout the speciman, $F(\langle R \rangle)$ decreases to zero with a Gaussian-like tail. The "bits" from the successive 0.7 μ sec. pulses are not perfectly additive because the walls, at cut-off, settle into the nearest position of minimum energy. This experiment confirms the idea that the shape of the second maximum in the "switching time curve" is determined by the distribution of nucleation centers through the function $F(\langle R \rangle)$.

The sharp peaks which occur at rise-time and cut-off are, like the first maximum in the "switching time curve", due primarily to reversible flux changes. There is a considerable contribution, however, from the creation or acceleration of the irreversibly moving walls during rise-time and the return of these walls to their nearest potential minimum at cut-off. This latter contribution will be larger the larger the area of irreversibly moving wall. The sharp peaks which occur at rise-time should reach, therefore, a maximum when the irreversibly moving wall area is a maximum, or F ($<R>$) is a maximum. In agreement with this model, the rise-time peaks have a maximum in the same 0.7 μ sec. pulse in which the "bit" corresponding to irreversible wall motion is a maximum. The maximum in the cut-off peak occurs somewhat earlier. This is attributed to the fact that irreversibly growing walls collide with both reversibly and irreversibly moving walls. Collisions of the former type hold the reversibly moving wall so that at cut-off it can no longer move to contribute a flux change. The number of reversibly created and growing domains is significantly reduced before the irreversibly moving wall area is a maximum, and their proportional contribution to the peak is larger at "cut off" than "rise-time". Only those irreversibly moving walls which move back to a potential minimum contribute to the "cut off" peak.

Eq. (25) can be written in the form $H_m = S_w/\tau - H_o$. A measurement of H_m vs. $1/\tau$ should yield a straight line relationship with intercept $H_o \approx H_c$ and slope S_w. This relationship will hold only for $H_m > H_c$ but not so large as to make the rise-time of the input pulse a large fraction of the switching time. Measurements of H_m vs. $1/\tau$ are shown in Figs. 9 and 10, respectively, for a 4-79 Mo-Permalloy, 1/8 mil, grain oriented ribbon core and a General Ceramic MF 1326 B magnesium-manganese ferrite ($\sim$ 20-20-60) body. The measurements of Fig. 10 were taken by R. Freeman of Group 63. Both curves are straight lines in agreement with theory.

The measured values of H_o are 0.14 Oe. and 1.0 Oe. respectively as compared with saturation coercivities of $\sim$0.15 Oe. and $\sim$1.5 Oe. A quantitative calculation of S_w cannot be made since not all of the material parameters have been directly measured. However, an order of magnitude can be obtained for comparison with the slope of the curves in Figs. 9 and 10.

For 1/8 mil metal tapes $\rho < \cos\theta > > R_m$. The switching coefficient is, by Eqs. (22), (24), and (25),

$$S_w \cong \left\{ \frac{\rho I_s \Lambda \sqrt{k_1/A}}{(\Lambda^2 + \gamma^2 I_s^2) \langle \cos\theta_i \rangle} + \frac{8\pi^2 I_s R_m^2}{\rho_e c^2 \langle \cos^2\theta_i \rangle \langle \cos\theta_i \rangle} \right\}, \qquad (27)$$

$$A = 2kT_c S^2 / a^2.$$

For 4-79 Mo-Permalloy $I_s \sim 700$ gauss and $T_c = 730^\circ$K. Since it is a grain oriented material, $\langle \cos\theta_i \rangle \approx 1$. The tape thickness is 3.2×10^{-4} cm so that $R_m = 1.6 \times 10^{-4}$ cm. The resistivity is $\rho_e \approx 6 \times 10^{-17}$ e.s.u.-cm so that $S^e_w \sim 0.3 \times 10^{-7}$ Oe.-sec. The anisotropy constant for 80-20 nickel-iron is $|K_1| \approx 8 \times 10^3$ ergs/cm^3. This value is taken for 4-79 Mo-Permalloy. The exchange factor is $A \sim 10^{-6}$ ergs/cm and $\sqrt{|K_1|/A} \sim 10^5$ cm^{-1}. Although the relaxation frequency Λ is not known for 4-79 Mo-Permalloy, it has been measured as $\Lambda \approx 2 \times 10^8$ sec^{-1} in Supermalloy[13]. The gyromagnetic ratio is $\gamma \approx 2 \times 10^7$ (gauss-sec.)$^{-1}$. Since ρ is the distance a domain wall travels in the time τ, and since it is believed that some grain boundaries will nucleate at most one domain of reverse magnetization, the distance ρ should be approximately an average grain diameter or $\rho \sim 5 \times 10^{-3}$ cm. Then

$$\rho \Lambda \sqrt{|K_1|/A} / \gamma^2 I_s \sim 4 \times 10^{-7} \text{ Oe.-sec.}$$

which is larger than the eddy current contribution by a factor of 10. The eddy currents are not, apparently, what limits the rapidity with which a metallic ribbon core can switch. The calculated switching parameter is, therefore, S_w (calc) $\sim 4 \times 10^{-7}$ Oe.-sec. as compared with a measured value S_w (expt.) $= 5.5 \times 10^{-7}$ Oe.-sec. The close agreement between theory and experiment depends, of course, on the somewhat arbitrary choice of $\rho \sim 5 \times 10^{-3}$ cm. This is as reasonable a figure as could be chosen for ρ.

The General Ceramic ferrite MF 1326 B has an $I_s \approx 140$ gauss. The distance $\rho / \langle \cos\theta_2 \rangle \sim 5 \times 10^{-3}$ cm or a typical dimension of a grain. Preliminary

---

13. C. Kittel, J. Phys. et Radium, 12, 291 (1951)

reports by D. Epstein of the L.I.R. laboratories of M.I.T. indicate that the anisotropy constant for the magnesium-manganese ferrites is low. The value $|K_1| \sim 5 \times 10^3$ ergs/cm^3 is taken. The exchange parameter is $A \sim 10^{-6}$ ergs/cm and $\sqrt{|K_1|/A} \sim 7 \times 10^4$ cm^{-1}. The relaxation frequency is not known. The value $\Lambda \sim 10^8$ sec^{-1} is again taken. The eddy current effect is ignored and since $\Lambda^2 << I_s^2 \gamma^2$, S_w (calc.) $\cong \Lambda \sqrt{|K_1|/A} / I_s \gamma^2 \sim 6 \times 10^{-7}$ Oe.-sec. The value of S_w as measured from the slope of the line in Fig. 10 is S_w(expt) = 5.7×10^{-7} Oe.-sec. Again it should be emphasized that the excellent agreement between theory and experiment result from the somewhat arbitrary selection of $\rho \sim 5 \times 10^{-3}$cm. The agreement does show, however, that the theory is reasonable.

Summary.

A model of nucleation of domains of reverse magnetization at grain boundaries with subsequent growth to saturate the sample has been proposed for the "switching" mechanism in magnetic cores. This model predicts square hysteresis loops for polycrystalline materials with aligned directions of easy magnetization from grain to grain. It further predicts that reasonably square minor loops may be obtained in materials of low saturation magnetization and small grain size without an alignment of the directions of easy magnetization.

The shape of the "switching time curve" is explained on the basis of this model. The switching time τ is calculated in terms of measurable parameters. The relationship $H_c \tau \approx S_w$ for optimum operating conditions shows that a compromise must be made between H_c and τ. In order to lower the parameter S_w, three lines of attack suggest themselves. The first is to decrease ρ by decreasing the grain size of the material so as to increase the grain boundary surface area. The second is to study what factors affect the relaxation frequency Λ. This parameter appears to vary by a factor of 10^2 between different materials at room temperature. A third would be to obtain as low an anisotropy constant K_1 as is consistant with the requirements of hysteresis loop squareness.

Finally the eddy current effects have been shown to be small compared to the relaxation effect in determining the switching time in both metal-tape and ferrite cores.

Signed John B. Goodenough
John B. Goodenough

Norman Menyuk
Norman Menyuk

Approved DRB 9K.
David R. Brown

JBG/NM:jk:jrt

Drawings Attached:

Figure 1 and 2	A-54071
Figure 3	A-54057
Figure 4	A-54058
Figure 5	A-54059
Figure 6	A-54100
Figure 7	A-54061
Figure 8	A-54072
Figure 9	A-54073
Figure 10	A-54070

(20)

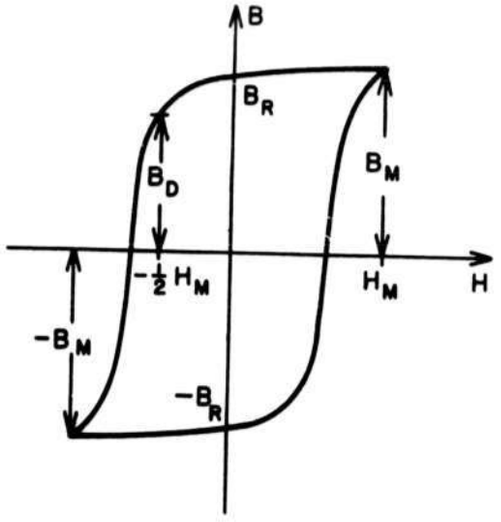

FIGURE 1

SCHEMATIC DYNAMIC SQUARE HYSTERESIS LOOP FOR A MAGNETIC CORE DRIVEN BY A PEAK DRIVING CURRENT I_M

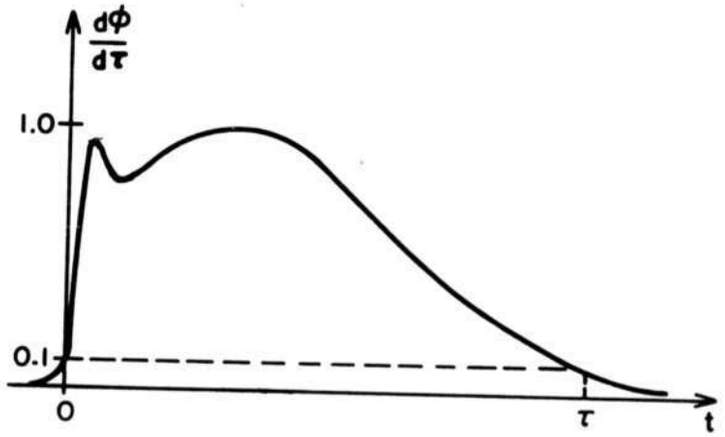

FIGURE 2

SCHEMATIC OUTPUT SIGNAL FOR A SLOW SWITCHING CORE. TWO MAXIMA ARE APPARENT.

A-54071

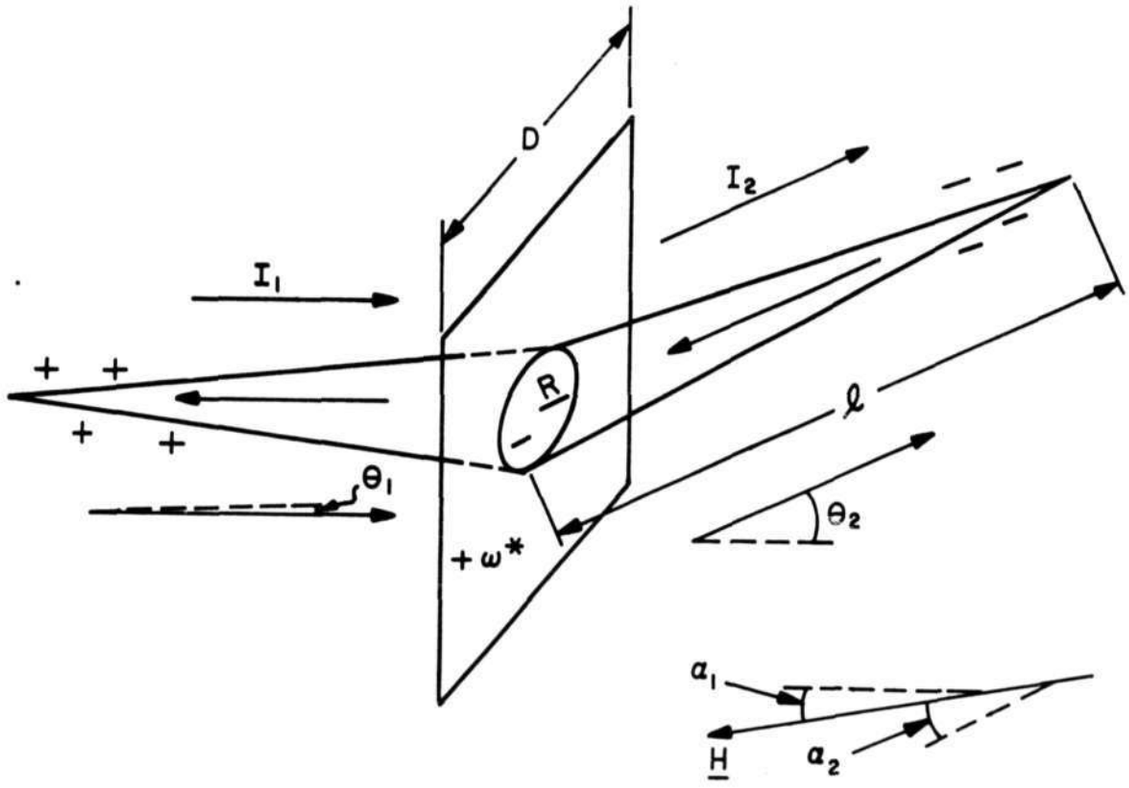

FIG. 3
SCHEMATIC NUCLEATION OF A
DOMAIN OF REVERSE MAGNETIZATION
AT A GRAIN BOUNDARY

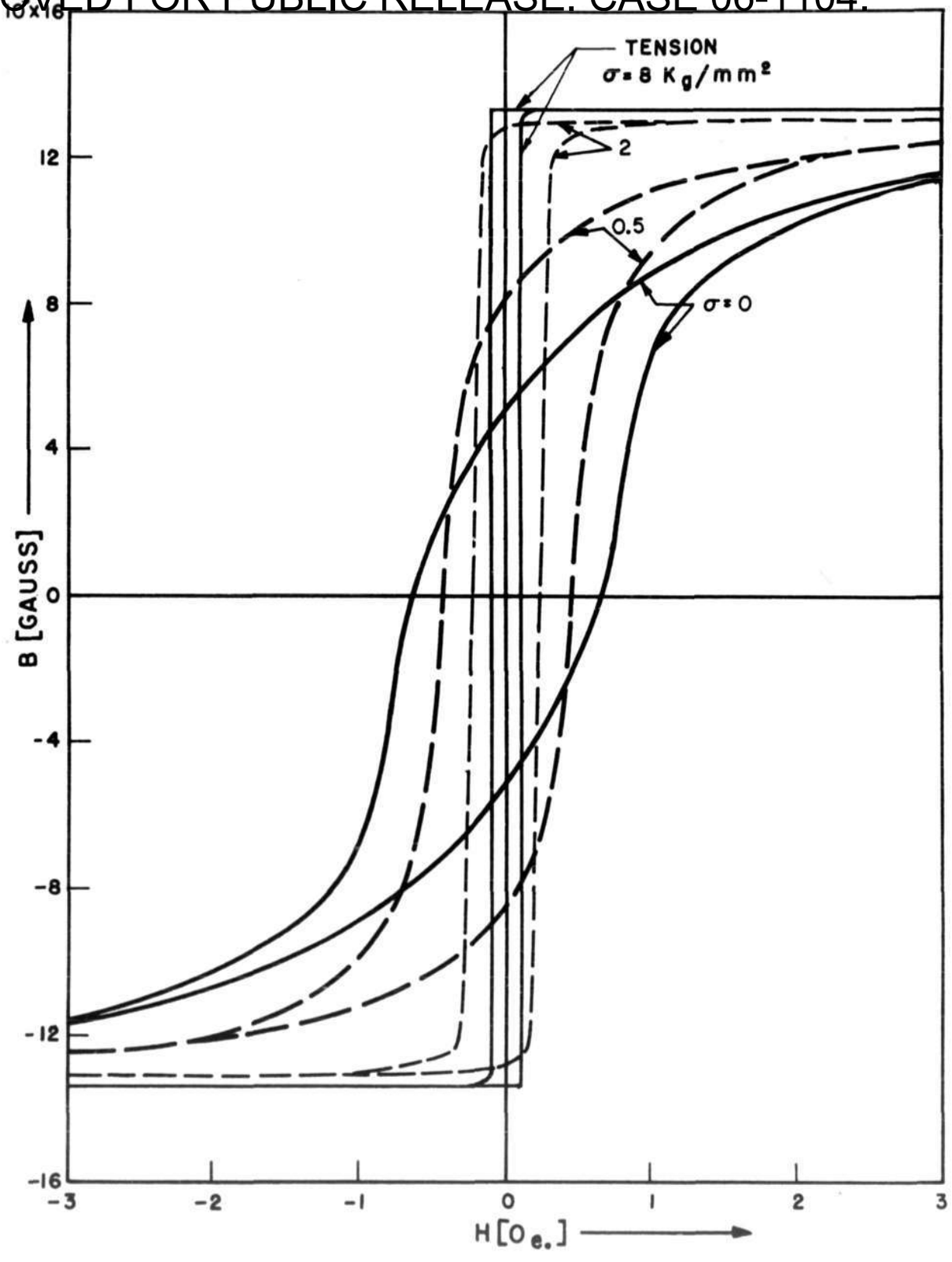

FIG. 4
HYSTERESIS LOOPS OF
68 PERMALLOY UNDER TENSION.
MAXIMUM FIELD STRENGTH 5 OERSTEDS

A-54058

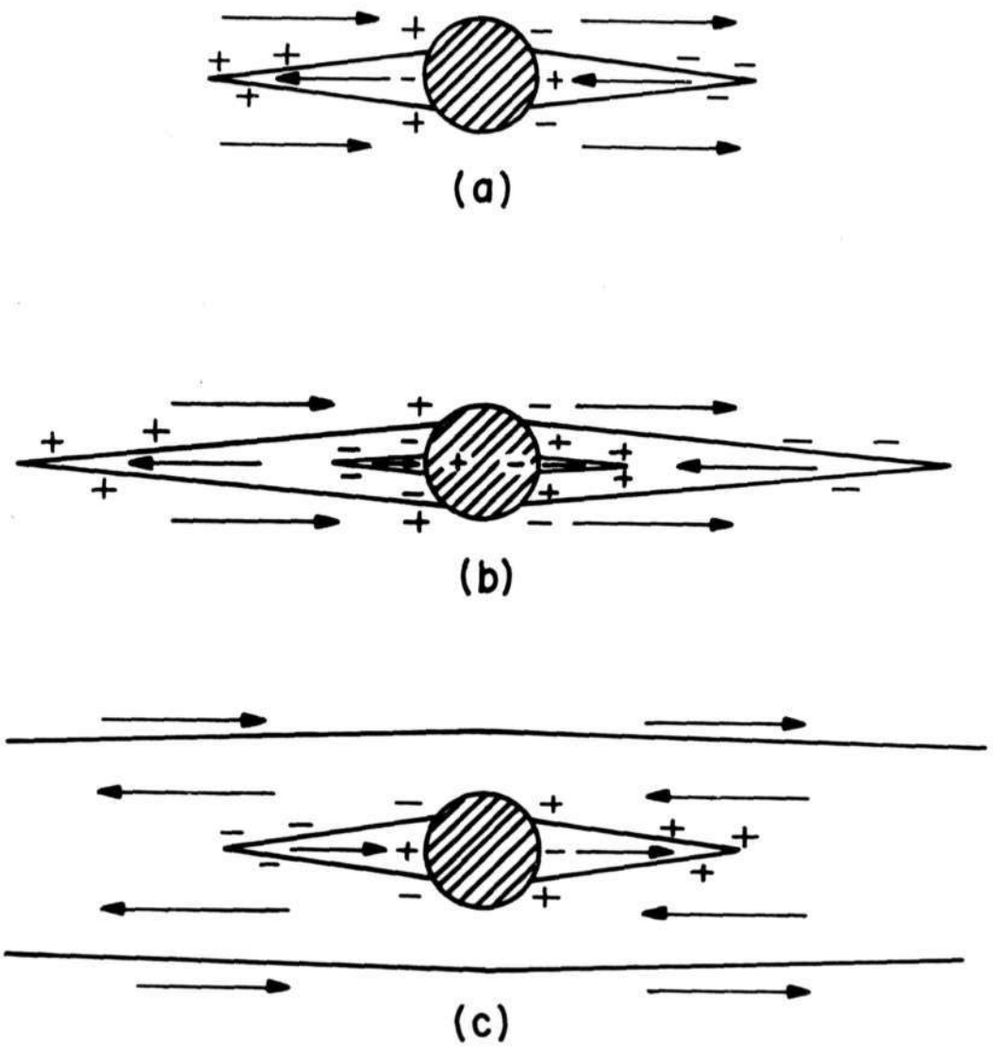

FIG. 5

SCHEMATIC REPRESENTATION OF GROWTH OF A DOMAIN OF REVERSE MAGNETIZATION AWAY FROM AN INCLUSION IN A PARALLEL EXTERNAL FIELD H. THE CRYSTAL HAS BUT ONE AXIS OF EASY MAGNETIZATION

A-54059

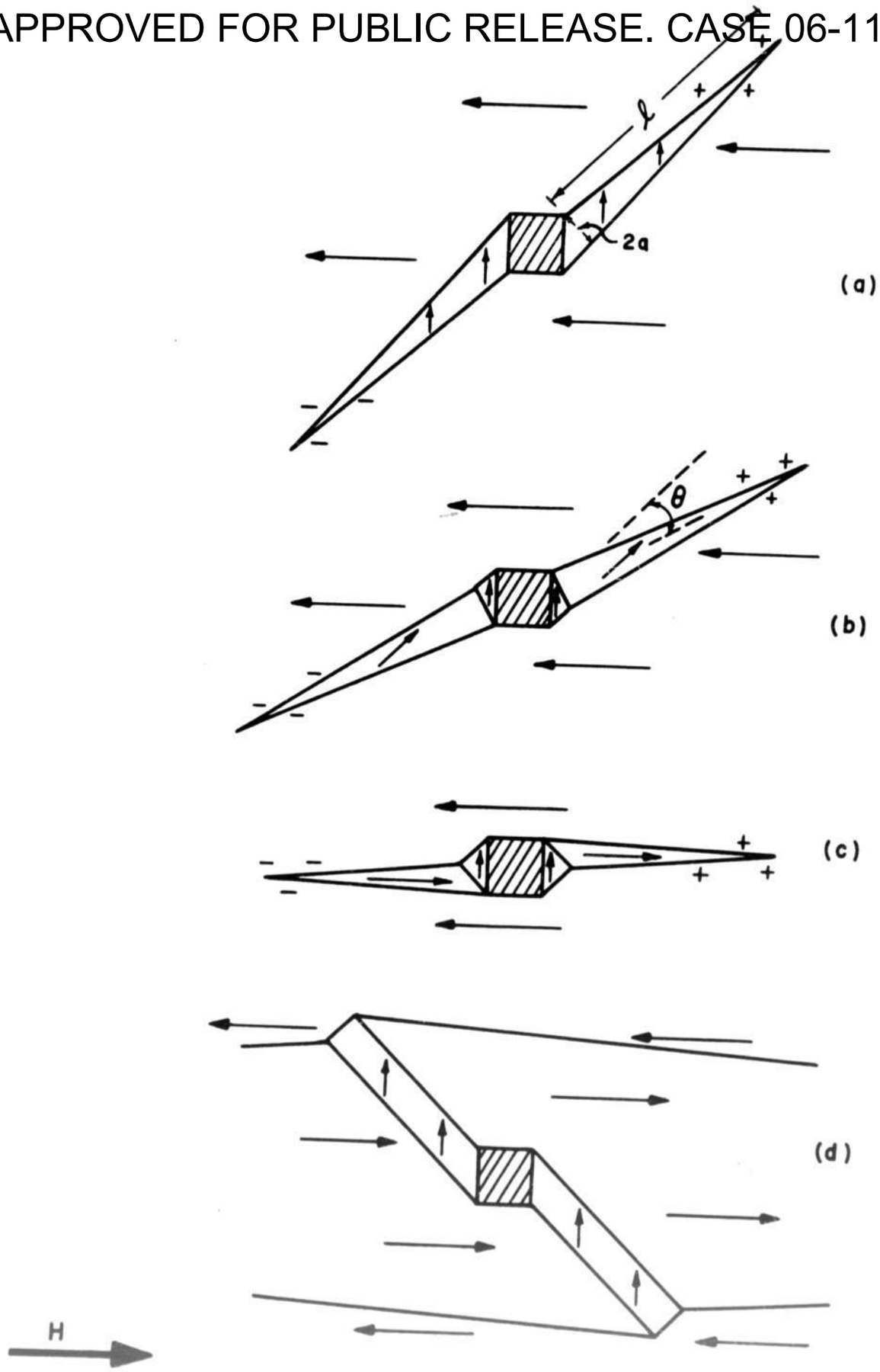

FIG. 6

CREATION AND GROWTH OF A DOMAIN OF REVERSE MAGNETIZATION BY THE ROTATION OF A CLOSURE DOMAIN AT AN INCLUSION

A-54100

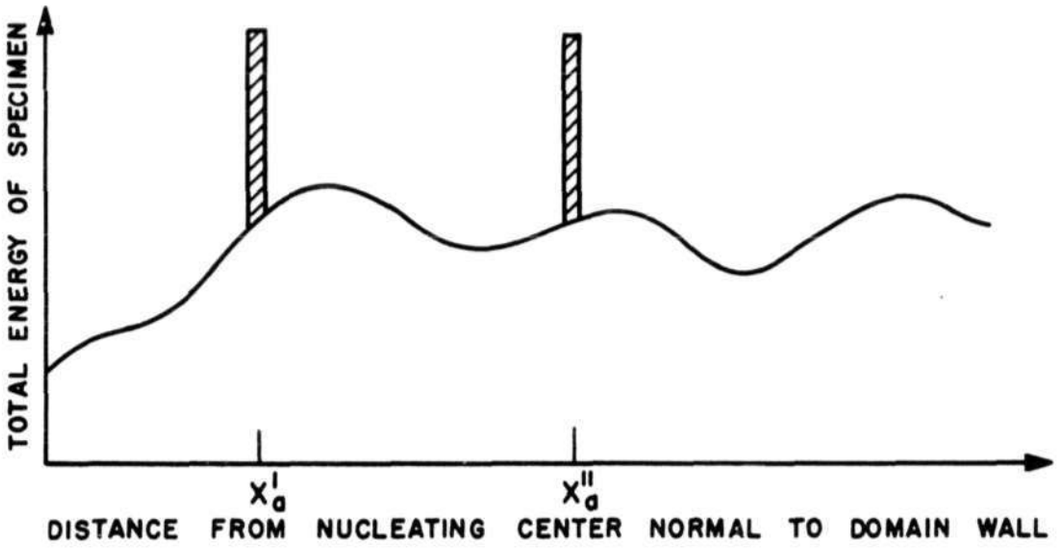

(a) CORRESPONDS TO REVERSIBLE NUCLEATION

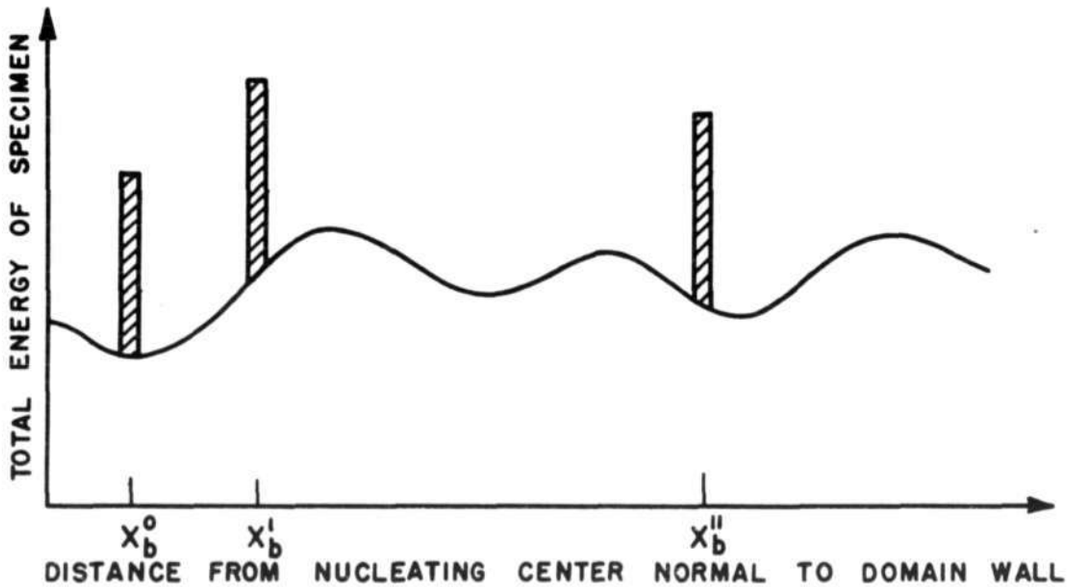

(b) CORRESPONDS TO IRREVERSIBLE NUCLEATION

FIG. 7

SCHEMATIC POTENTIAL ENERGY CURVES AS A FUNCTION OF POSITION OF THE DOMAIN WALL IN THE CRYSTAL LATTICE WHEN $H_N < H_C$

A-54061

SWEEP TIME 6 μSEC/CM

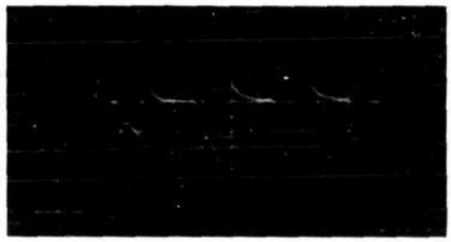

SWEEP TIME 1 μSEC/CM

FIGURE 8

OUTPUT VOLTAGE vs TIME FOR A ROLLED, $\frac{1}{8}$ MIL Mo-PERMALLOY CORE DRIVEN BY ONE LONG PULSE FOLLOWED BY A SERIES OF OPPOSITE 0.7 μSEC PULSES

A-54072

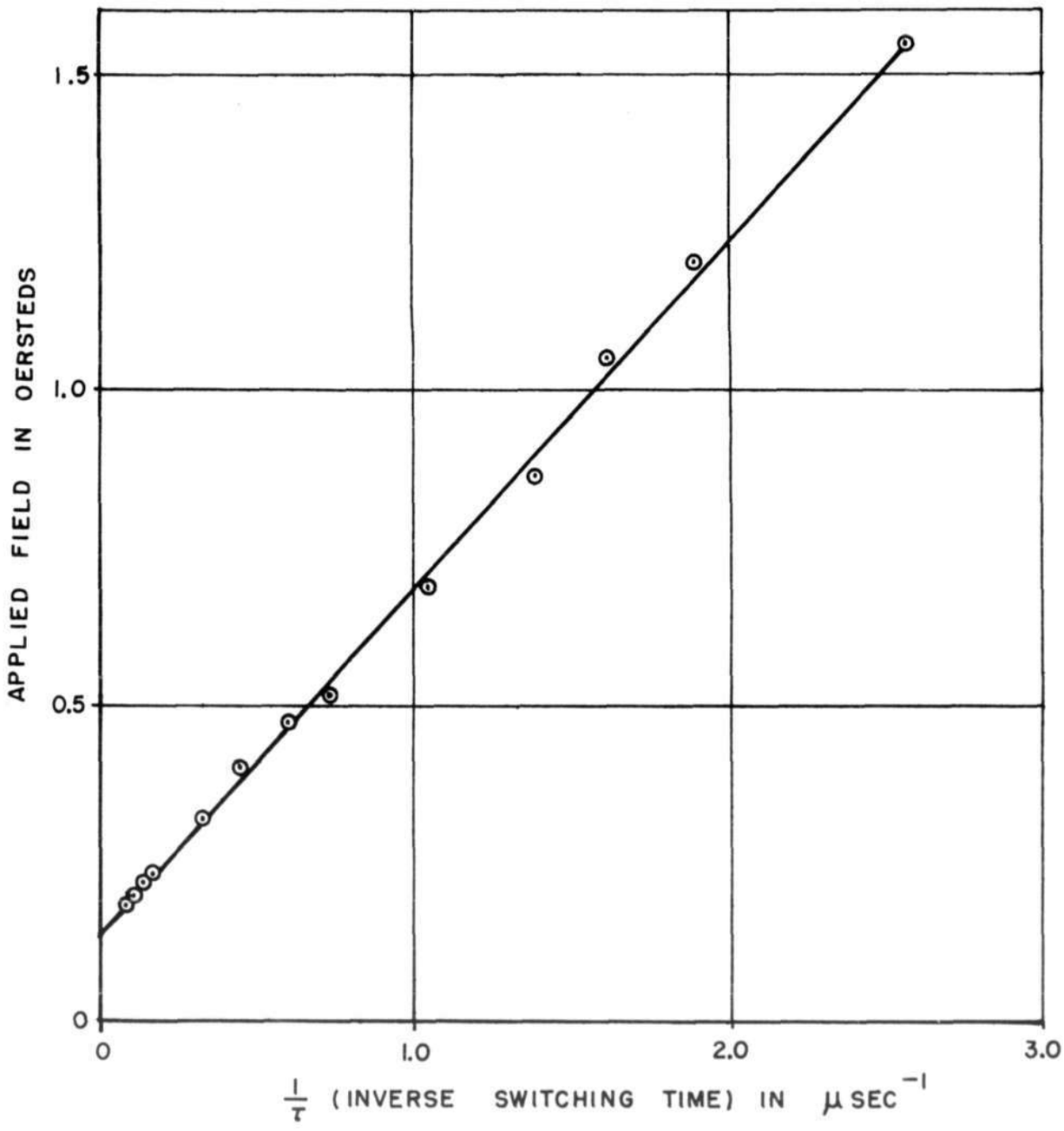

FIGURE 9

MEASUREMENT OF H_M vs $\frac{1}{\tau}$ FOR A 4-79 Mo-PERMALLOY RIBBON CORE ROLLED TO $\frac{1}{8}$ MIL THICKNESS

A-54073

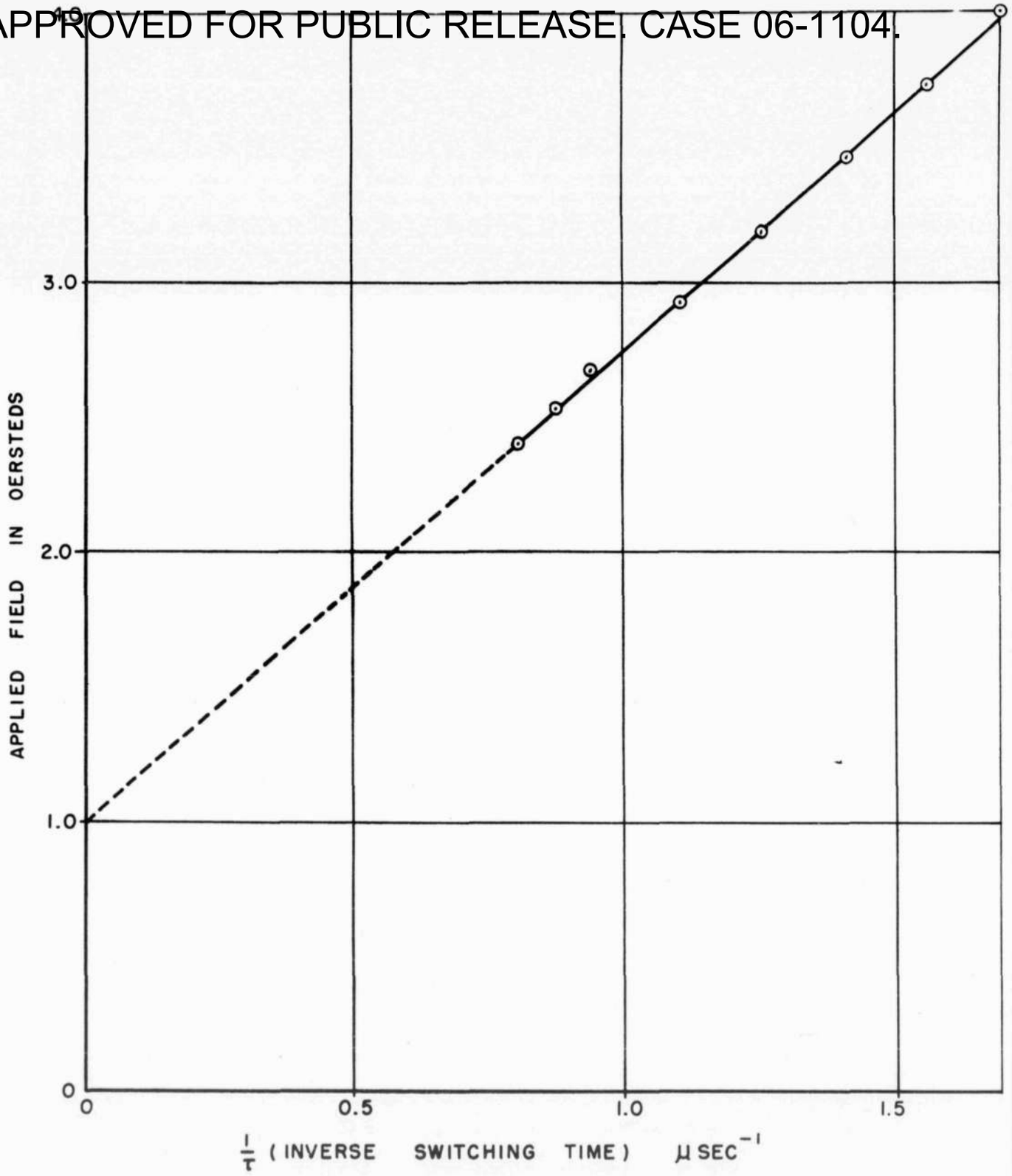

FIGURE 10
MEASUREMENT OF H_M vs $\frac{1}{\tau}$ FOR
GENERAL CERAMIC MF-1326 CORE

A-54070